Manuscript Details

Manuscript number	CSTE_2019_2290
Title	3D Microwave Printing Temperature Control of Continuous Carbon Fiber Reinforced Composites
Article type	Full Length Article

Abstract

Continuous carbon fibers show dramatic promise as reinforcement materials to improve the stiffness, strength properties and design ability of 3D printed polymer parts. However current 3D printing methods have a very slow printing speed because the intrinsic slow and contact needed heat transfer disadvantages of the traditional resistive heating approach. We present a 3D microwave printing method by using the microwave for instantaneous and volumetric heating the continuous carbon fiber reinforced polymer (CCFRP) filament. This allows fabricating CCFRP components with much faster speed and higher printing amount compare with the traditional 3D printing technologies. To utilize the benefit of fast printing speed, the speed-variation 3D microwave printing is applied to adapt the diverse printing path and reduce the printing period. In this paper, a 3D microwave printing temperature control method by combining the prediction-model and step-proportional-integral-derivative control is researched to reduce the printing temperature difference of the CCFRP filaments during the speed-variation printing process. Three different CCFRP specimens with variation printing speed are compared, including a spanner, an aircraft and a spider from Nazca lines. The experimental results indicate that the new printing temperature control method for 3D microwave printing process dramatically reduces the temperature deviation. This technology solved a key problem of 3D microwave printing of continuous carbon fiber reinforced polymer composites and can be used to manufacture complex polymer-matrix composite materials.

Keywords	Microwave processing; 3D printing; Carbon fibres; Polymer-matrix composites (PMCs).
Manuscript category	Energy and functional composites
Manuscript region of origin	Asia Pacific

Corresponding Author	Nanya Li
Corresponding Author's Institution	Karlsruhe Institute of Technology
Order of Authors	Nanya Li, Guido Link, John Jelonnek

Suggested reviewers	Dong Lin, Chad Duty, Ryosuke Matsuzaki, Weilong Cong, Tian Xiaoyong, Wai Yee Yeong, Wenzheng Wu

Submission Files Included in this PDF

File Name [File Type]

Cover letter.doc [Cover Letter]

Manuscript.doc [Manuscript File]

Figure 1.tif [Figure]

Figure 2.tif [Figure]

Figure 3.tif [Figure]

Figure 4.tif [Figure]

Figure 5.tif [Figure]

Figure 6.tif [Figure]

Supplementary Information.doc [Supplementary Material]

Submission Files Not Included in this PDF

File Name [File Type]

3DMP_Video.mp4 [Video]

To view all the submission files, including those not included in the PDF, click on the manuscript title on your EVISE Homepage, then click 'Download zip file'.

August 25, 2019

Dear Editors,

We would like to submit our manuscript titled **"3D Microwave Printing Temperature Control of Continuous Carbon Fiber Reinforced Composites"**
by Nanya Li, Guido Link, John Jelonnek
for possible publication in
COMPOSITES SCIENCE AND TECHNOLOGY

The significance of this paper for the research community can be summarized as the following:

(1) The current 3D printing process of continuous fiber reinforced polymer composite has a very slow printing speed because the intrinsic slow and contact needed heat transfer disadvantages of the traditional resistive heating approach. We present a 3D microwave printing method by using the microwave for instantaneous and volumetric heating the continuous carbon fiber reinforced polymer composite. This allows fabricating composite materials with much faster speed and higher printing amount compare with the traditional 3D printing technologies.

(2) Different from the traditional 3D printing, the 3D microwave printing temperature has a strong relationship with the printing speed. The relationship between the printing temperature and the speed is revealed and established the prediction-model in this manuscript.

What it contains that is most important and new can be summarized as the following:

(1) The 3D microwave printing temperature control method by combining the prediction-model and step-proportional-integral-derivative control is researched to reduce the printing temperature difference of the composite filaments during the speed-variation printing process.

(2) The experiment results exhibited that the new method dramatically reduces the standard deviation of the printing temperature to 66%, 56%, 60% of the composite spanner, aircraft and Nazca lines spider respectively, by comparing with general PID control method.

Thank you for your patient help and support.

Sincerely,

Dr. Nanya Li
Institute for Pulsed Power and Microwave Technology
Karlsruhe Institute of Technology, Eggenstein-Leopoldshafen, 76344, Germany
Email: nanya.li@kit.edu
Phone: +49 721 608-23620

3D Microwave Printing Temperature Control of Continuous Carbon Fiber Reinforced Composites

Nanya Li*, Guido Link, John Jelonnek

Institute for Pulsed Power and Microwave Technology, Karlsruhe Institute of Technology, Eggenstein-Leopoldshafen, 76344, Germany
*Corresponding authors (Nanya.li@kit.edu)

Abstract

Continuous carbon fibers show dramatic promise as reinforcement materials to improve the stiffness, strength properties and design ability of 3D printed polymer parts. However current 3D printing methods have a very slow printing speed because the intrinsic slow and contact needed heat transfer disadvantages of the traditional resistive heating approach. We present a 3D microwave printing method by using the microwave for instantaneous and volumetric heating the continuous carbon fiber reinforced polymer (CCFRP) filament. This allows fabricating CCFRP components with much faster speed and higher printing amount compare with the traditional 3D printing technologies. To utilize the benefit of fast printing speed, the speed-variation 3D microwave printing is applied to adapt the diverse printing path and reduce the printing period. In this paper, a 3D microwave printing temperature control method by combining the prediction-model and step-proportional-integral-derivative control is researched to reduce the printing temperature difference of the CCFRP filaments during the speed-variation printing process. Three different CCFRP specimens with variation printing speed are compared, including a spanner, an aircraft and a spider from Nazca

Institute for Pulsed Power and Microwave Technology (IHM), Karlsruhe Institute of Technology, 76344 Eggenstein-Leopoldshafen, Germany.

Dr. Nanya Li: nanya.li@kit.edu

lines. The experimental results indicate that the new printing temperature control method for 3D microwave printing process dramatically reduces the temperature deviation. This technology solved a key problem of 3D microwave printing of continuous carbon fiber reinforced polymer composites and can be used to manufacture complex polymer-matrix composite materials.

Keywords: Microwave processing; 3D printing; Carbon fibres; Polymer-matrix composites (PMCs).

1 Introduction

3D printing, also known as additive manufacturing, has been studied for more than 20 years for potential application in aerospace [1], automotive and medical treatment [2]. Benefit from the computer-aided design, numerical and automatic control, the three-dimensional (3D) printing, known as additive manufacturing through material extrusion, is a burgeoning method for manufacturing of composite materials and already leads to a revolution in the manufacturing industry.

The mostly used printing technologies for composite materials include direct ink writing [3], fused filament fabrication (FFF) [4-6], stereolithographic printing [7] and laminated object manufacturing [8]. Recently, the authors [9] researched the continuous carbon fiber reinforced thermoplastic composite printing by in-nozzle impregnation of FFF printing process and indicated that by introducing the continuous carbon fiber, the extrusion process turns into pultrusion. Matsuzaki et al. [10] mixed the continuous carbon fiber and polylactic resin to fabricate fiber reinforced composites which showed mechanical properties much better than the unreinforced thermoplastics. Caminero M. A. et al. [11] demonstrated that the impact strength and interlaminar shear strength exhibited by 3D printed continuous carbon fiber reinforced Nylon composites were higher than the usual 3D printed samples. Hou Z. [12] et al. showed that the average specific strength of 3D printed continuous Kevlar fiber reinforced polylactide composite was comparable with the corrugated-core sandwich composite fabricated by traditional processes. The tensile and flexural strength of 3D printed specimens were tested, and the results exhibited that the loads were transferred from matrix to fibers [13]. By using the infrared heating, the surface temperature of the printed layer are increased and can improve the interlayer strength of the printed parts [14]. The authors also [15] developed a free-hanging 3D printing method to manufacture continuous carbon fiber reinforced thermoplastic lattice truss core structures. However, the printing speed of current 3D printing technologies of CCFRP still limited to 7 mm/s. Ye et al. printed the continuous carbon fiber reinforced thermoplastic polyimide composite at a speed of 5 mm/s [16]. The company Markforged published the Mark series 3D printer and the printing speed during fabricating continuous fiber reinforced polymer parts is only about 7 mm/s [17].

The described research works employed the traditional resistive heater to heat the filament during the printing process. During the printing process, the thermal heat transfer from heating block to the fiber is obstructed by the resin which has low heat conductivity coefficient. This limits the printing speed. If the printing speed is too high, the core area of the filament may still be below melting temperature. Increasing the heat flow by an increase of the heating block temperature is limited by the degradation temperature of the filament. As a result, the traditional 3D printing method can only manufacture small end-use products with extremely low printing speed and efficiency.

Due to the drawbacks of contact heat transfer caused slow printing speed and non-uniform heating, we proposed the 3D microwave printing (3DMP) method of continuous carbon fiber reinforced thermoplastic composites with higher printing speed and performance. The first 3D microwave printer SERPENS (Super Efficient and Rapid Printing by Electromagnetic-heating Necessitated System) has already been developed by the authors. Based on this 3D microwave printing prototype, the microwave heating temperature control methods under variation printing speed are researched. The printing temperature deviation of three different CCFRP specimens, including a spanner, an aircraft and a spider from Nazca lines, is compared by using different temperature control methods. The spanner has long straight printing path, the aircraft specimen contains sharp corners and lots of complex curves exist in the spider specimen. At last, the optical diagrams of the 3D microwave printed specimens are investigated.

2 Materials and Methods

2.1 Materials used and the 3D microwave printer SERPENS

The 1K 66tex HT T300 carbon fiber (Toray Industries) and 910 nylon material (Taulamn3D, melting temperature: 210 ^{o}C) were applied in this paper. The PA845H-PL nylon sizing agent (Michelman company) was used for the surface modification of the continuous carbon fiber bundle. The self-developed continuous carbon fiber impregnation system and 3D microwave printer SERPENS are applied, as shown in Fig. S1 to Fig. S3 in the supplementary information.

2.2 Investigation of 3DMP temperature control methods

A FLIR A35 infrared thermal camera was applied to measure the temperature of the CCFRP filament inside the resonant cavity during microwave heating. The fast 60 Hz monitoring frequency of the camera makes sure the filament temperature can be captured precisely during the printing process. The temperature control strategy can be divided into two stages, the first stage is to heat the filament from room temperature to the printing temperature, and the second stage is to maintain the melting temperature under different printing speed. For the first stage, general proportional-integral -derivative (PID) control will be employed to adjust the microwave power and increase the filament temperature. The main challenge of the 3DMP temperature control is the second stage, which needs to control the microwave power corresponding to the printing speed. The different temperature control methods for the second stage are investigated, including the general PID, fixed microwave power, step-PID (output step-function signals) and the combination of prediction-model and step-PID control methods, as illustrated in Fig. 1. The general PID control has temperature feedback from the infrared camera and controls the microwave output power by pulse-width modulation (PWM), as shown in Fig. 1 (a). By using the PWM control signal, the microwave power generated from the solid-state microwave amplifier can be precisely adjusted with 0.1 W resolution continuously. The fixed microwave power control provides a constant microwave power during the printing process and does not relate with the variation of printing speed, as shown in Fig. 1 (b). By modifying the general PID, step-PID is developed with a step-function control of the output signal. That means the microwave power will remain constant if the measured printing temperature has a slight fluctuation (±10 ^{o}C). The combination of prediction-model and step-PID control (PMSP) method is shown in Fig. 1 (c). The prediction-model based controller has the ability to adjust the microwave power before the changing of printing speed (Detailed information is described in Fig. S4 of the supplementary information). The temperature deviation of different printing path with variation printing speed is compared and researched.

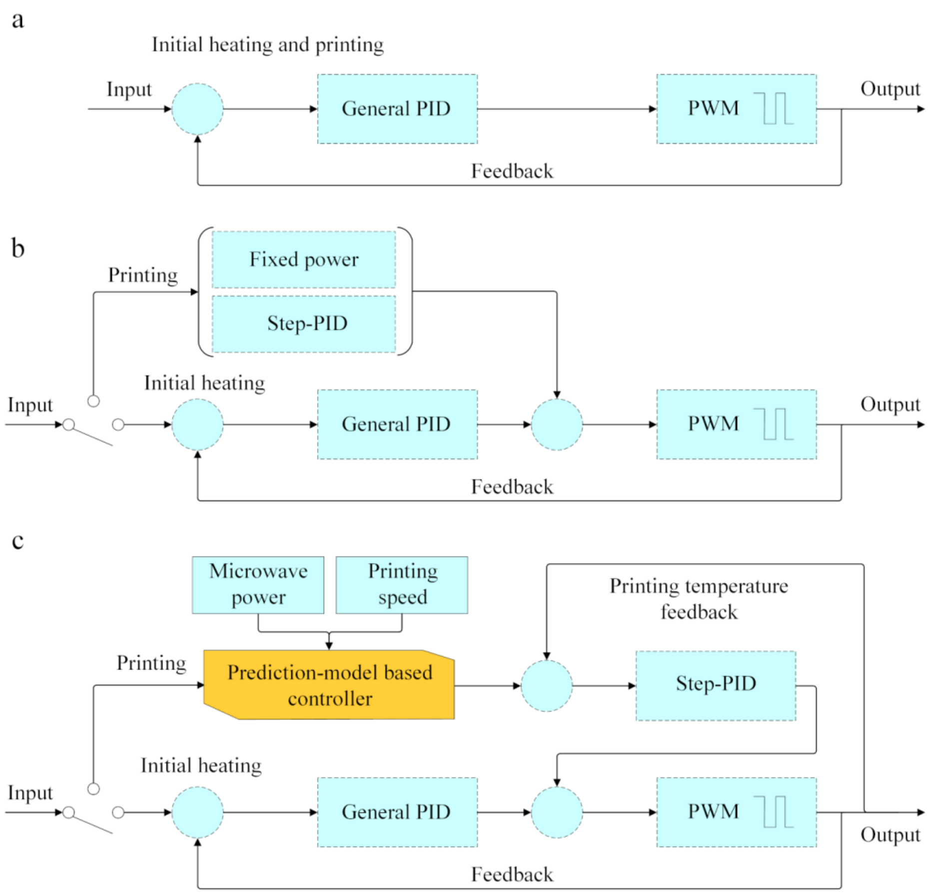

Fig. 1. 3D microwave printing temperature control methods of CCFRP, (a) general PID control for initial heating and printing process, (b) fixed microwave power and step-PID controlled printing process, (c) prediction-model and step-PID (PMSP) control method.

3 Results and Discussion

3.1 3D microwave printing temperature control of CCFRP

Based on the SERPENS 3D microwave printing system, the microwave heating power of continuous carbon fiber reinforced nylon filaments are measured under different printing speed, as shown in Fig 2. The fluctuation of the measured microwave power may be caused by the varying position of the 0.45 mm diameter filament in the 2 mm diameter nozzle tube. The relationship between microwave power and the printing speed can be expressed as: $P = 10.5 + 0.5 \times V$. Where P is microwave power (W) and V is printing speed (mm/s). For a motionless filament in the microwave applicator, only about 10.5 W microwave power is needed to heat the filament to 210 ^{o}C. The microwave power increases along with the increasing of printing speed, as illustrated in Fig. 2 (a). The testing device is shown in Fig. S8 in the supplementary information. In order to control the printing speed, the output signal from the Megatronics control board is measured and recorded along with the printing speed, as shown in Fig. 2 (b). Before the printing process, the G-code will be revised to insert the command to output the speed control signal. The control signal will be adjusted according to printing speed and the microwave amplifier always start to change the power earlier than the changing of printing speed.

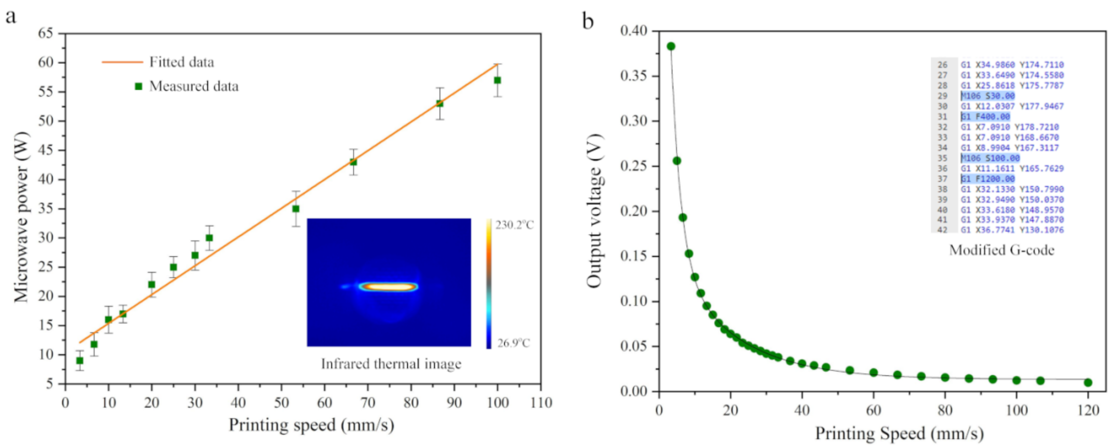

Fig. 2. Relationship between microwave power and printing speed, (a) measured microwave power at different printing speed and linear fit, (b) relationship between step motor signal and printing speed.

To validate the efficiency of the 3D microwave printing temperature control method, three different specimens with variation printing speed is printed, including a spanner, an aircraft and a spider from Nazca lines (a biomorphic graph in the shape of a spider) [18]. In principle, the 3DMP method is a pultrusion process, rather than an extrusion process. Because the continuous carbon fibers are pulled out from the microwave applicator and bond to the printing bed continuously. If the printing path has a changing direction vector (such as a curve or turning corner), a persistent bonding force from the previous printed filament section is needed. Thus, the straight printing path has the direction vectors in one direction and can achieve the highest printing speed. But the curves or turning corners should apply a low speed to make sure the filament can bond to the printing bed. The printing path with variation printing speed was generated by calculating the radius of curvatures of curves and the angles between direction vectors of the path. The code was programmed in Matlab and the algorithm information is described in the supplementary information (Table S1).

As illustrated in Fig. 3 (a), the radius of curvatures of the printing path are calculated (the calculated angles between the adjacent direction vectors are informed in Fig. S5 in the supplementary information). The different color point out the magnitude of the direction vectors and the arrows indicate the changing direction. After that, the printing speed diagram is achieved, the light red areas have a printing speed of 20 mm/s, and the blue areas are 7 mm/s, as shown in Fig. 3 (b). It is obvious that the turning, corner and round areas have the 7 mm/s printing speed and the straight and large curvature areas have the 20 mm/s printing speed. The measured printing temperature and microwave power of different printing temperature control methods are exhibited from Fig. 3 (d) to (h). It can be seen that the microwave has a very fast heating rate of the filament, and before the start of the printing process, a dwell stage at 210 ^{o}C is applied.

Obviously, the highest temperature difference of the CCFRP filament occurred when the fixed microwave power is imposed during the printing process. That is the first key difference between the traditional resistive heating 3D printing and the 3D microwave printing technology, constant heating power is failed for 3DMP. The filament temperature is very sensitive to the microwave power inputted in the applicator, due to the strong microwave absorption properties of continuous carbon fiber. Fig. 3 (e) and (f) exhibit the curves of printing temperature and power under general PID and step-PID control methods. A similar standard deviation (in short of SD in the figure and indicates the dispersion degree of the printing temperature) of the printing temperature is measured of these two control methods, which is 44.3 ^{o}C and 47.6 ^{o}C respectively. Finally, the printed CCFRP spanner by using PMSP control method is shown in Fig. 3 (c). By comparing the printing temperature and the printing path, we found that the highest temperature difference occurs on the notched corner of the spanner, which is the speed changing areas.

Even if a small standard deviation is obtained compared with the fixed power control method, a large maximum temperature value during the step-PID printing process can be discovered, as shown in Fig. 3 (i). Because, no matter how fast the temperature feedback is of the PID controller, it always delays to the changing of the printing speed, a strong regulation signal will generate and may cause overshoot of temperature. This is the second key difference between the traditional 3D printing and the 3D microwave printing technology, ex-post PID control methods (the widely used heating method in traditional 3D printing) lack of control ability of the 3DMP. Therefore, the new prediction-model based temperature control method is presented in this paper and shown in Fig. 3 (g) and (h). A tremendous advance of the 3D microwave printing temperature control is implemented and the measured data show small temperature variation and standard deviation, as illustrated in Fig. 3 (i). The instantaneous change of microwave power happens when the printing speed change from one to another. For this CCFRP spanner, 8 high-speed and 7 low-speed paths are calculated, which correspond to 8 peaks and 7 troughs of the square wave shown in Fig. 3 (g). Due to the random communication delay (about 0.2 s to 0.25 s) between the MatLab control code and the microwave amplifier, sometimes the microwave power control could not correspond to the printing speed (about 0.02 s to 0.05 s leading or lagging). As a result, the step-PID is introduced to work with the prediction-model based controller to reduce the influence of random communication delay, as shown in Fig. 3 (h). The standard deviation of prediction-model and step-PID (PMSP) control method reduces by 69% and 26% of the step-PID and prediction-model control method, respectively. The PMSP method dramatically reduces the standard deviation of printing temperature by 73% and 66% of the fixed power and general PID method, respectively.

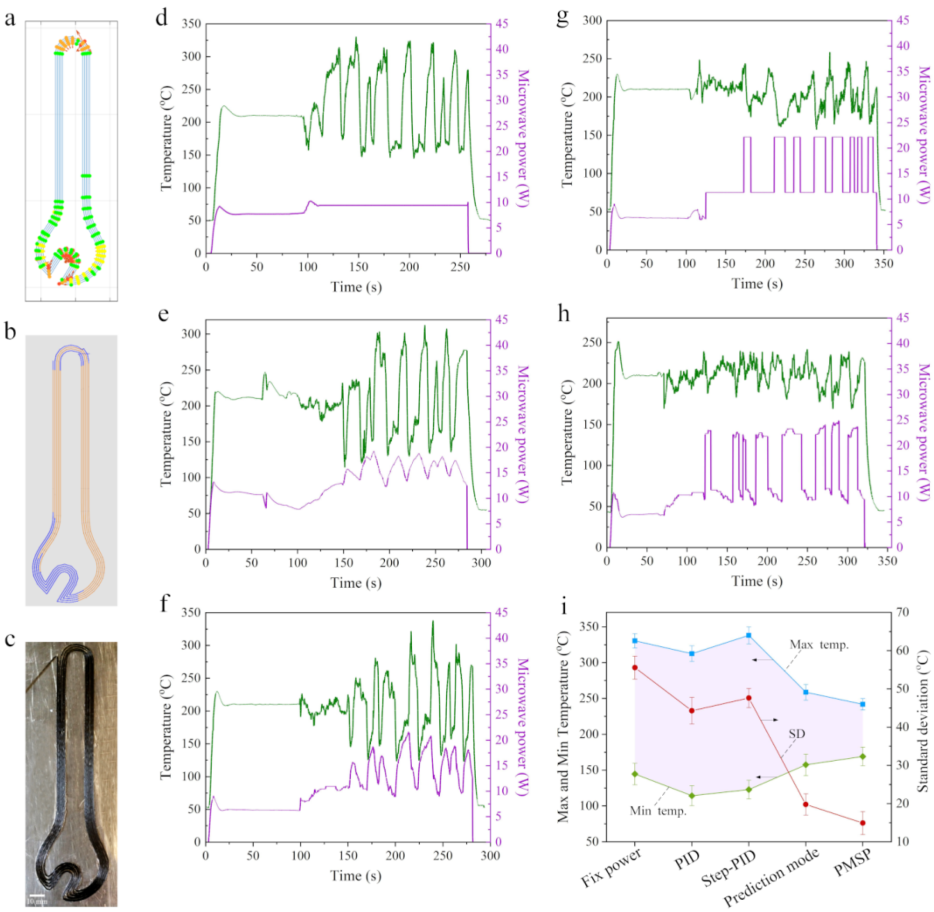

Fig. 3. 3D microwave printed CCFRP spanner and measured printing temperature during the printing process, (a) calculated radius of curvatures of the printing path, (b) printing speed variation along the printing path of the spanner, (c) the printed CCFRP spanner by PMSP method, (d) printing temperature under fixed microwave power, (e) printing temperature under general PID controlled microwave power, (f) printing temperature under step-PID controlled microwave power, (g) printing temperature under prediction-model controlled microwave power, (h) printing temperature under prediction-model and step-PID controlled microwave power, (i) the comparison of five different printing temperature control methods.

In Fig. 4, a CCFRP aircraft is printed by 3DMP and the five different printing temperature control methods are applied to analyze the temperature difference. Compare with the spanner, the aircraft has many small angles between the straight lines. That means the variation of printing speed is more frequent than the spanner. To utilize the fast printing advantages of 3DMP, the yellow areas also have a printing speed of 20 mm/s, and the blue areas are 7 mm/s. As the measurement results of the spanner, the printing temperature controlled by fixed power shows a regular variation tendency, which follows the changing of printing speed, as shown in Fig. 4 (d). For the general PID and step-PID control methods, the standard deviation (SD) of temperature reduced compare with the fixed power control method. However, the measured maximum and minimum temperature are even worse than the fixed power control method, as shown in Fig. 4 (e), (f) and (i). Because the ex-post PID control leads to that the high speed already switches to low speed, but the microwave power still maintains at high level and may even keep increasing. Therefore, the standard deviation, maximum and minimum printing temperature of prediction-model control methods are much lower than the fixed power, general PID and step-PID methods. Furthermore, by using the PMSP control method, the standard deviation reduces by 53% of fixed power, 56% of general PID and 51% of step-PID methods, as shown in Fig. 4 (h) and (i).

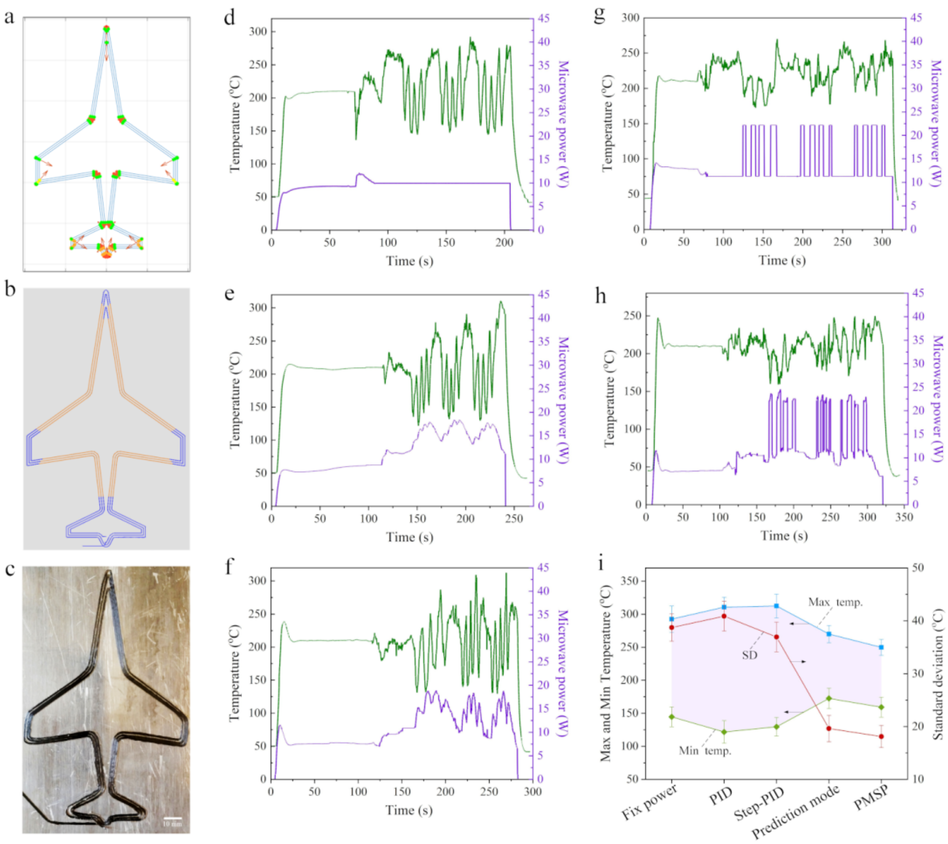

Fig. 4. 3D microwave printed CCFRP aircraft and measured printing temperature during the printing process, (a) calculated radius of curvatures of the printing path, (b) printing speed variation along the printing path of the spanner, (c) the printed CCFRP aircraft by PMSP method, (d) printing temperature under fixed microwave power, (e) printing temperature under general PID controlled microwave power, (f) printing

temperature under step-PID controlled microwave power, (g) printing temperature under prediction-model controlled microwave power, (h) printing temperature under prediction-model and step-PID controlled microwave power, (i) the comparison of five different printing temperature control methods.

Another complex CCFRP part with lots of curves and corners are shown in Fig. 5, and this biomorphic spider shape comes from the Nazca lines [18], and three different printing speed are applied, including 20 mm/s (yellow areas), 13 mm/s (green areas) and 7 mm/s (blue areas), as illustrated in Fig. 5 (b). The measured printing temperature controlled by fixed power method shows high-temperature fluctuation during the printing process, as shown in Fig. 5 (d). Furthermore, the temperature difference increases due to the low-temperature filament cannot bond to the printing bed on the sharp corners. The fixed power control method for this complex spider part has a standard deviation of 44 ^{o}C, but the standard deviation (SD) of the PMSP temperature control method is only 18 ^{o}C. Finally, the standard deviation further reduces by 53% and 34% compared with the step-PID and prediction-model based control method, by using the PMSP control method, as shown in Fig. 5 (h) and (i). The CCFRP spider printed by the PMSP temperature control method is illustrated in Fig. 5 (c).

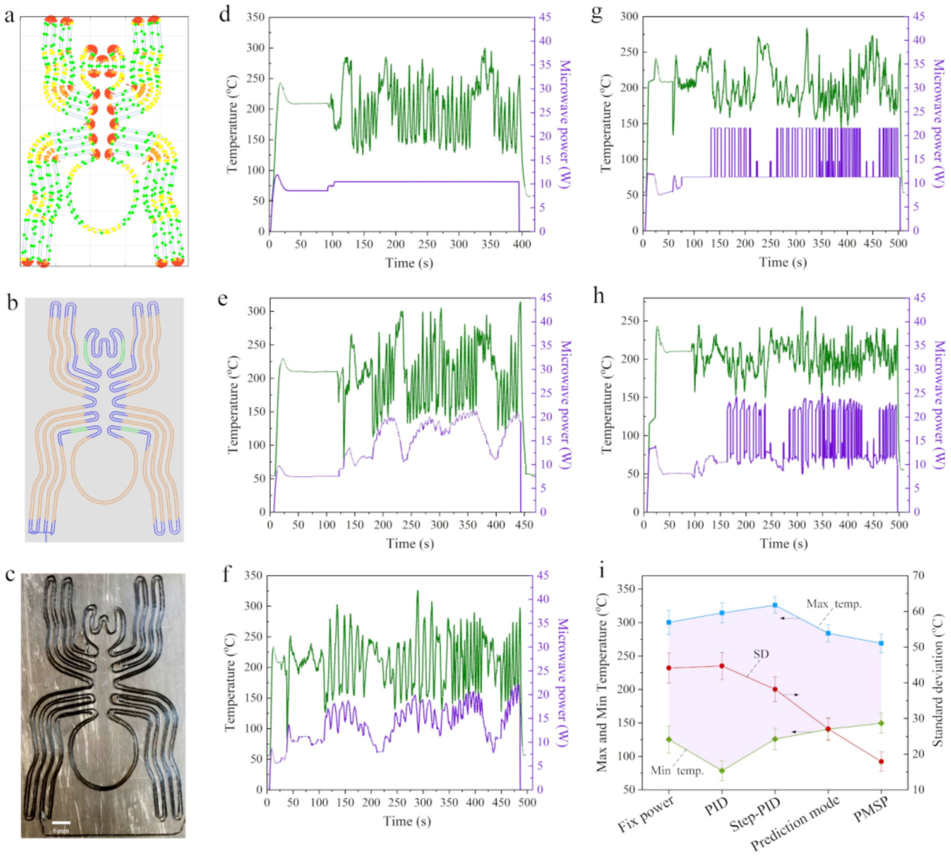

Fig. 5. 3D microwave printed CCFRP Nazca lines spider and measured printing temperature during the printing process, (a) calculated radius of curvatures of the printing path, (b) printing speed variation along the printing path of the spanner, (c) the printed CCFRP Nazca lines spider by PMSP method, (d) printing temperature under fixed microwave power, (e) printing temperature under general PID controlled microwave power, (f) printing temperature under step-PID controlled microwave power, (g) printing temperature under prediction-model controlled microwave power, (h) printing temperature under prediction-model and step-PID controlled microwave power, (i) the comparison of five different printing temperature control methods.

3.2 Optics inspection of 3D microwave printed CCFRP

As illustrated in Fig. 6, the 3D microwave printing technology can print different CCFRP shapes with variation printing speed. All of these optical figures have the same size bar shown in Fig. 6 (a). It is obvious that after the round filaments were heated by microwave and printed on the platform, the filaments change the shape to flat strip, as shown in the cross-section figures of the printed specimen in Fig. S9 of the supplementary information. Consequently, the strip-filament has better bonding strength to each other and avoids the voids between them. From Fig. 6 (a) to (c), the straight lines, curved lines and arc turning corner have the printing speed of 20 mm/s. Under a high printing speed, the filaments still can follow the printing path (yellow dash lines) and have very less disordered carbon fibers, because of the rapid and volumetric microwave heating. Due to the strong stiffness of the carbon fiber bundle, the folding of the strip-filament on a sharp corner is expected as shown in Fig. 6 (e) and (f). Even the direction vectors of the 180 ^{o} circular corner and sharp angle corners are changing persistently, the volumetric microwave heating and lower printing speed ensure the filament can be printed, as shown in Fig. 6 (d) to (f).

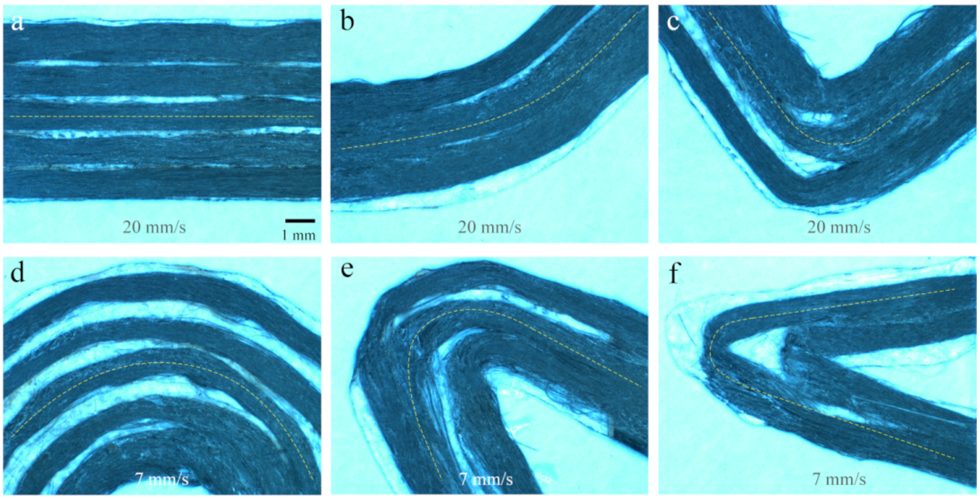

Fig. 6. Zoomed optical figures of 3D microwave printed CCFRP with different speed and shapes, (a) straight lines, (b) curved lines, (c) arc turning corner, (d) 180 ^{o} circular corner, (e) 75 ^{o} corner. (f) 23 ^{o} corner.

4 Conclusions

The less efficient heat transfer of conventional heating leads to the slow printing speed, small printing amount and low heating temperature. On the contrary, the microwave has rapid energy radiation, volumetric, selective and uniform heating advantages. In this paper, we present a 3D microwave printing temperature control method under variation printing speed on a 3D microwave printing platform named SERPENS. A prediction-model and step-PID (PMSP) combined method has been presented and compared with other temperature control methods. The experiment results exhibited that the PMSP method dramatically reduces the standard deviation of the printing temperature to 66%, 56%, 60% of the CCFRP spanner, aircraft and Nazca lines spider respectively, by comparing with general PID control method. The ongoing project will use this technology to printing high-performance continuous carbon fiber reinforced polymer composites and develop the application object to more complex three-dimensional structures.

Acknowledgements

The authors would like to thanks the support of Alexander von Humboldt Foundation as well as to the donor, the German Federal Ministry for Education and Research. The authors also would like to thanks the programming by Mr. Ting Wang.

Reference

[1] G.D. Goh, S. Agarwala, G.L. Goh, V. Dikshit, S.L. Sing, W.Y. Yeong, Additive manufacturing in unmanned aerial vehicles (UAVs): Challenges and potential. Aerosp. Sci. Technol. 63 (2017) 140-151.

[2] P. Parandoush, D. Lin, A review on additive manufacturing of polymer-fiber composites, Compos. Struct. 182 (2017) 1-31.

[3] B.G. Compton, J.A. Lewis, 3D printing of lightweight cellular composites, Adv. Mater. 26 (2014) 5930-5935.

[4] J.P. Lewicki, J.N. Rodriguez, C. Zhu, M.A. Worsley, A.S. Wu, Y. Kanarska, J.D. Horn, E.B. Duoss, J.M. Ortega, W. Elmer, R. Hensleigh, 3D-Printing of meso-structurally ordered carbon fiber/polymer composites with unprecedented orthotropic physical properties, Sci. Rep. 7 (2017) 1-14.

[5] M. Invernizzi, G. Natale, M. Levi, S. Turri, G. Griffini, UV-assisted 3D printing of glass and carbon fiber-reinforced dual-cure polymer composites, Materials. 9 (2016) 1-12.

[6] F. Ning, W. Cong, J. Qiu, J. Wei, S. Wang, Additive manufacturing of carbon fiber reinforced thermoplastic composites using fused deposition modeling, Composites Part B, 80 (2015) 369-378.

[7] A.N. Dickson, J.N. Barry, K.A. McDonnell, D.P. Dowling. Fabrication of continuous carbon, glass and Kevlar fibre reinforced polymer composites using additive manufacturing, Addit. Manuf. 16 (2017) 146-152.

[8] S. Kumar, J. P Kruth, Composites by rapid prototyping technology, Mater. Des. 31 (2010) 850-856.

[9] N. Li, Y. Li, S. Liu, Rapid prototyping of continuous carbon fiber reinforced polylactic acid composites by 3D printing, J. Mater. Process. Technol. 238 (2016) 218-25.

[10] R. Matsuzaki, M. Ueda, M. Namiki, T.K. Jeong, H. Asahara, K. Horiguchi, T. Nakamura, A. Todoroki, Y. Hirano, Three-dimensional printing of continuous-fiber composites by in-nozzle impregnation. Sci. Rep. 11 (2016) 1-7.

[11] M.A. Caminero, J.M. Chacón, I. García-Moreno, G.P. Rodríguez, Impact damage resistance of 3D printed continuous fibre reinforced thermoplastic composites using fused deposition modelling, Composites Part B. 148 (2018) 93-103.

[12] Z. Hou, X. Tian, J. Zhang, D. Li, 3D printed continuous fibre reinforced composite corrugated structure, Compos. Struct. 184 (2018) 1005-1010.

[13] G. D. Goh, V. Dikshit, A.P. Nagalingam, G.L. Goh, S. Agarwala, S.L. Sing, J. Wei, W.Y. Yeong, Characterization of mechanical properties and fracture mode of additively manufactured carbon fiber and glass fiber reinforced thermoplastics, Mater. Des. 137 (2018) 1-11.

[14] V. Kishore, C. Ajinjeru, A. Nycz, B. Post, J. Lindahl, V. Kunc, C. Duty, Infrared preheating to improve interlayer strength of big area additive manufacturing (BAAM) components, Addit. Manuf. 14 (2017) 7-12.

[15] S. Liu, Y. Li, N. Li, A novel free-hanging 3D printing method for continuous carbon fiber reinforced thermoplastic lattice truss core structures, Mater. Des. 37 (2018) 235-244.

[16] W. Ye, G. Lin, W. Wu, P. Geng, X. Hu, Z. Gao, J. Zhao, Separated 3D printing of continuous carbon fiber reinforced thermoplastic polyimide, Composites Part A. 121 (2019) 457-464.

[17] L. G. Blok, M. L. Longana, H. Yu, B. K. Woods, An investigation into 3D printing of fibre reinforced thermoplastic composites, Addit. Manuf. 22 (2018) 176-186.

[18] H. Silverman, D. Browne, New evidence for the date of the Nazca lines. Antiquity. 65 (1991) 208-220.

Figure and Table Captions

Fig. 1. 3D microwave printing temperature control methods of CCFRP, (a) general PID control for initial heating and printing process, (b) fixed microwave power and step-PID controlled printing process, (c) prediction-model and step-PID (PMSP) control method.

Fig. 2. Relationship between microwave power and printing speed, (a) measured microwave power at different printing speed and linear fit, (b) relationship between step motor signal and printing speed.

Fig. 3. 3D microwave printed CCFRP spanner and measured printing temperature during the printing process, (a) calculated radius of curvatures of the printing path, (b) printing speed variation along the printing path of the spanner, (c) the printed CCFRP spanner by PMSP method, (d) printing temperature under fixed microwave power, (e) printing temperature under general PID controlled microwave power, (f) printing temperature under step-PID controlled microwave power, (g) printing temperature under prediction-model controlled microwave power, (h) printing temperature under prediction-model and step-PID controlled microwave power, (i) the comparison of five different printing temperature control methods.

Fig. 4. 3D microwave printed CCFRP aircraft and measured printing temperature during the printing process, (a) calculated radius of curvatures of the printing path, (b) printing speed variation along the printing path of the spanner, (c) the printed CCFRP aircraft by PMSP method, (d) printing temperature under fixed microwave power, (e) printing temperature under general PID controlled microwave power, (f) printing

temperature under step-PID controlled microwave power, (g) printing temperature under prediction-model controlled microwave power, (h) printing temperature under prediction-model and step-PID controlled microwave power, (i) the comparison of five different printing temperature control methods.

Fig. 5. 3D microwave printed CCFRP Nazca lines spider and measured printing temperature during the printing process, (a) calculated radius of curvatures of the printing path, (b) printing speed variation along the printing path of the spanner, (c) the printed CCFRP Nazca lines spider by PMSP method, (d) printing temperature under fixed microwave power, (e) printing temperature under general PID controlled microwave power, (f) printing temperature under step-PID controlled microwave power, (g) printing temperature under prediction-model controlled microwave power, (h) printing temperature under prediction-model and step-PID controlled microwave power, (i) the comparison of five different printing temperature control methods.

Fig. 6. Zoomed optical figures of 3D microwave printed CCFRP with different speed and shapes, (a) straight lines, (b) curved lines, (c) arc turning corner, (d) 180 ^{o} circular corner, (e) 75 ^{o} corner. (f) 23 ^{o} corner.

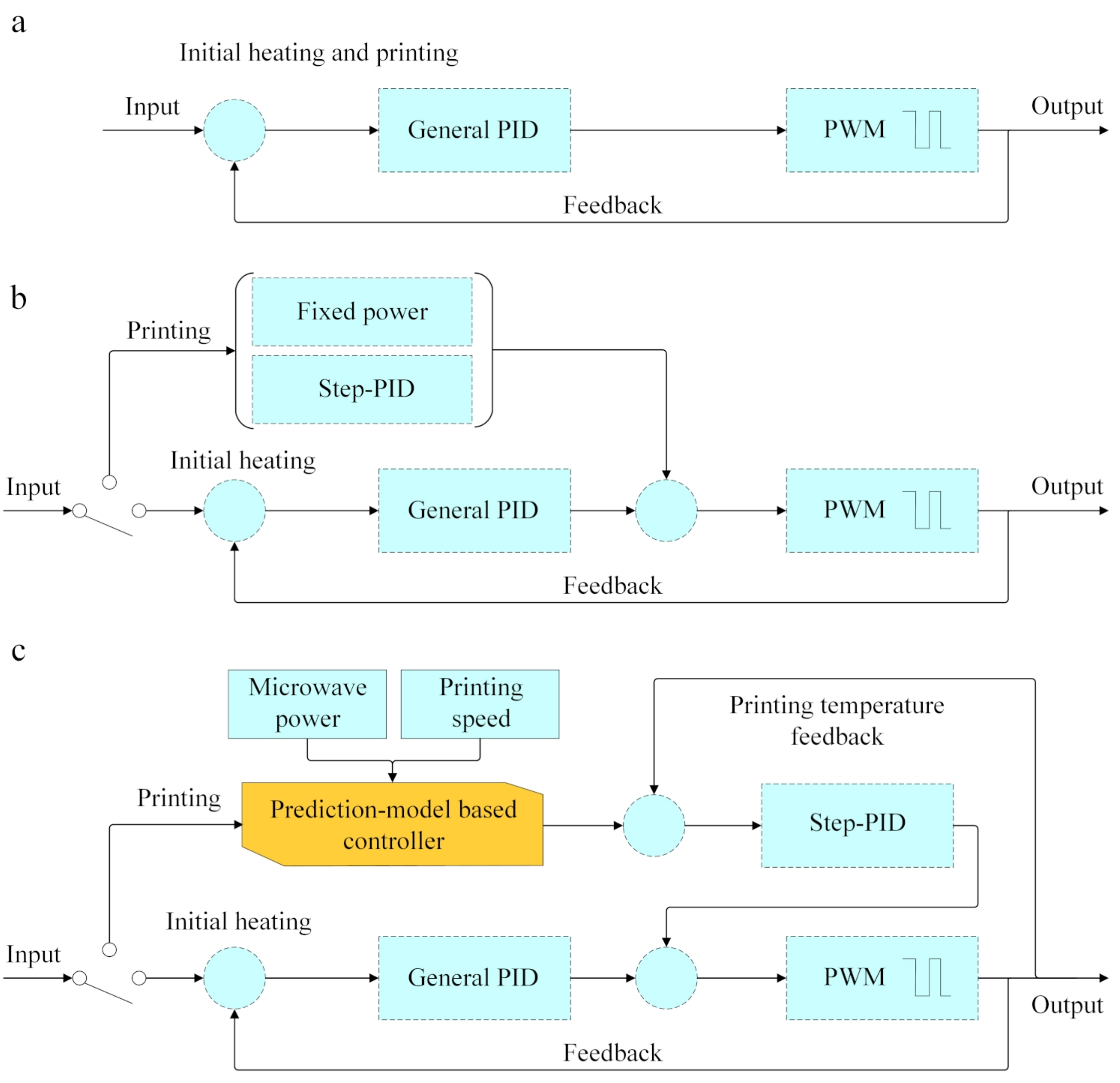

a
Initial heating and printing
Input
General PID
PWM
Output
Feedback
b
Printing
Fixed power
Step-PID
Initial heating
Input
General PID
PWM
Output
Feedback
c
Microwave power
Printing speed
Printing temperature feedback
Printing
Prediction-model based controller
Step-PID
Initial heating
Input
General PID
PWM
Output
Feedback

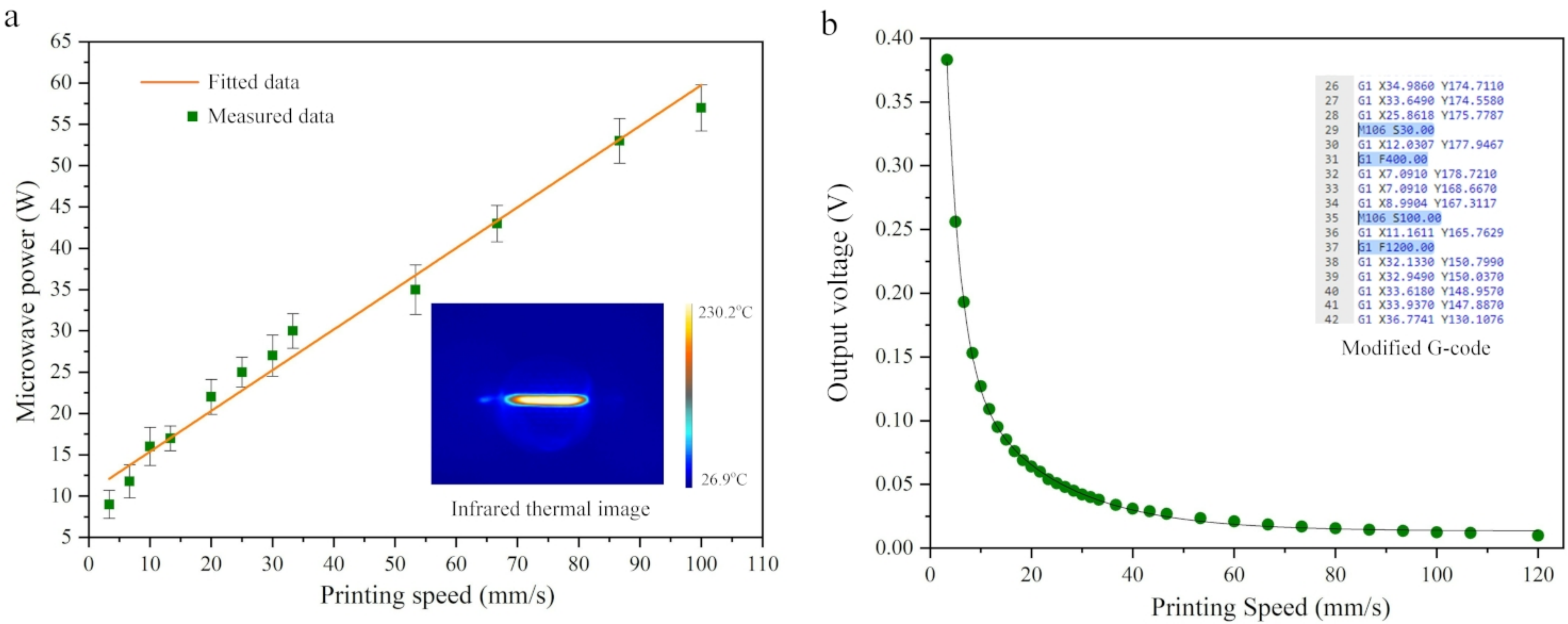
a
Microwave power (W)
Printing speed (mm/s)
Fitted data
Measured data
230.2°C
26.9°C
Infrared thermal image
b
Output voltage (V)
Printing Speed (mm/s)
26 G1 X34.9860 Y174.7110
27 G1 X33.6490 Y174.5580
28 G1 X25.8618 Y175.7787
29 M106 S30.00
30 G1 X12.0307 Y177.9467
31 G1 F400.00
32 G1 X7.0910 Y178.7210
33 G1 X7.0910 Y168.6670
34 G1 X8.9904 Y167.3117
35 M106 S100.00
36 G1 X11.1611 Y165.7629
37 G1 F1200.00
38 G1 X32.1330 Y150.7990
39 G1 X32.9490 Y150.0370
40 G1 X33.6180 Y148.9570
41 G1 X33.9370 Y147.8870
42 G1 X36.7741 Y130.1076
Modified G-code

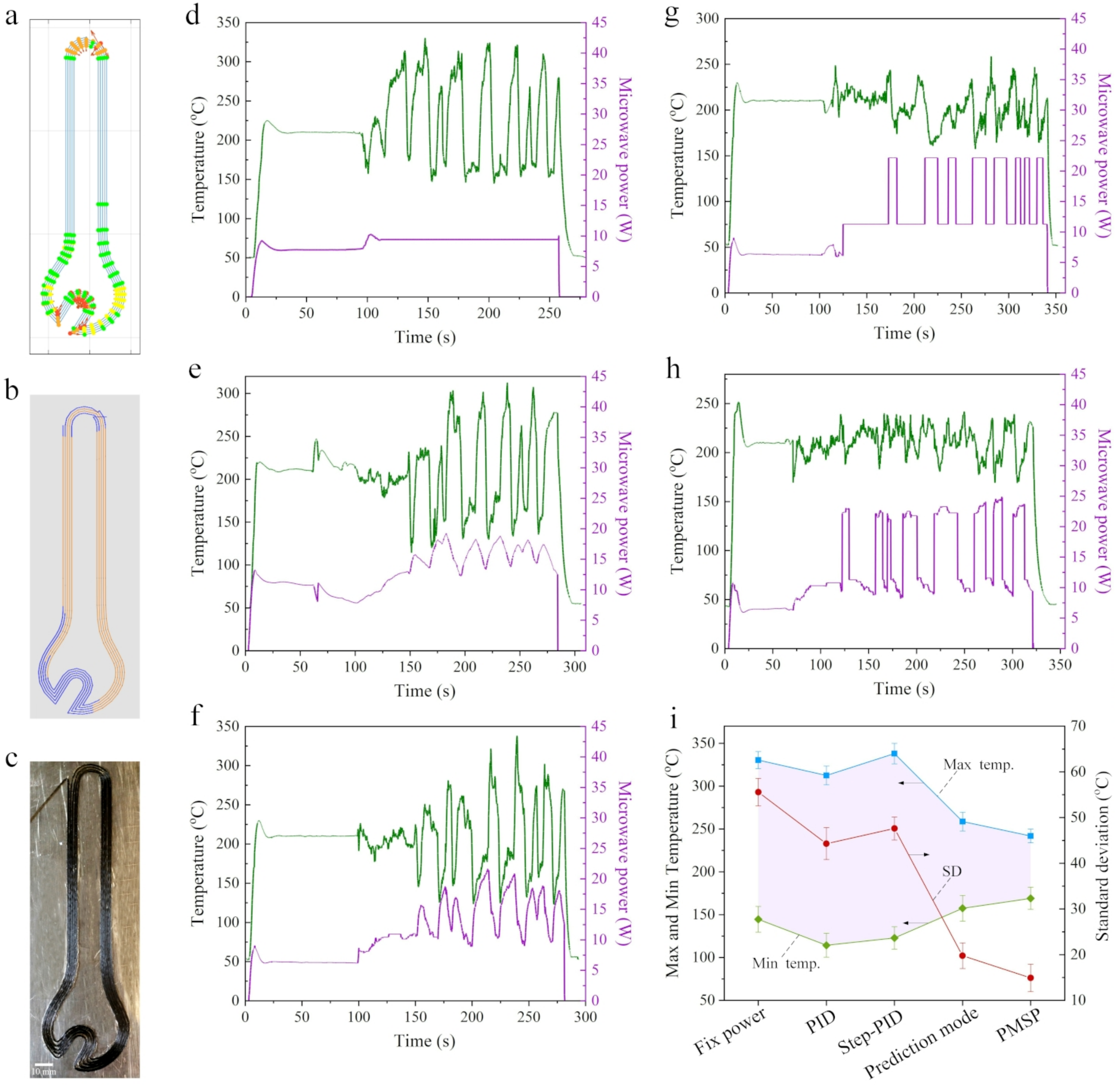

a
b
c
10 mm
d
e
f
g
h
i
Temperature (°C)
Microwave power (W)
Time (s)
Max and Min Temperature (°C)
Standard deviation (°C)
Max temp.
Min temp.
SD
Fix power
PID
Step-PID
Prediction mode
PMSP

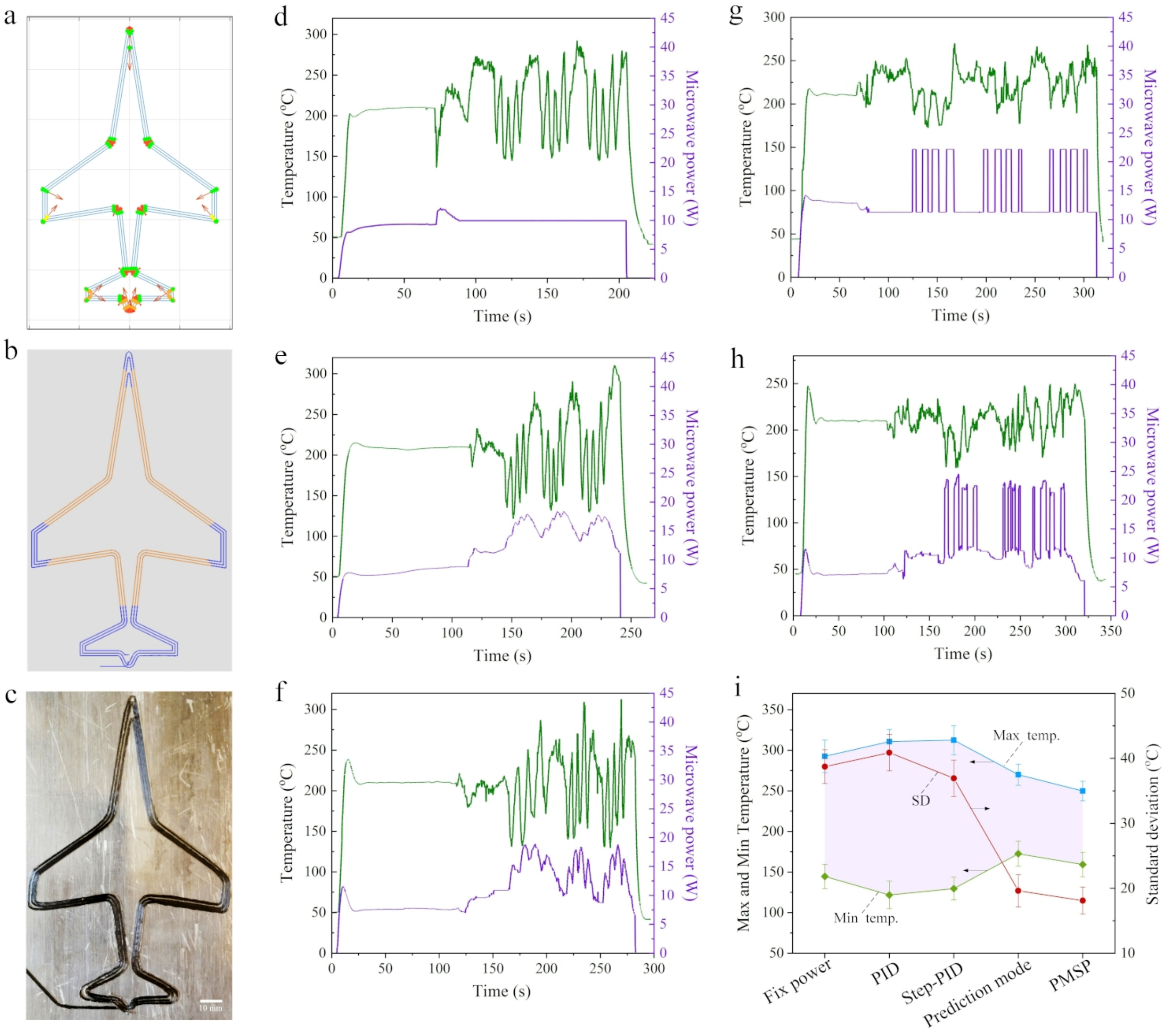
a
b
c
10 mm
d
e
f
g
h
i
Temperature (°C)
Microwave power (W)
Time (s)
Max and Min Temperature (°C)
Standard deviation (°C)
Max temp.
Min temp.
SD
Fix power
PID
Step-PID
Prediction mode
PMSP

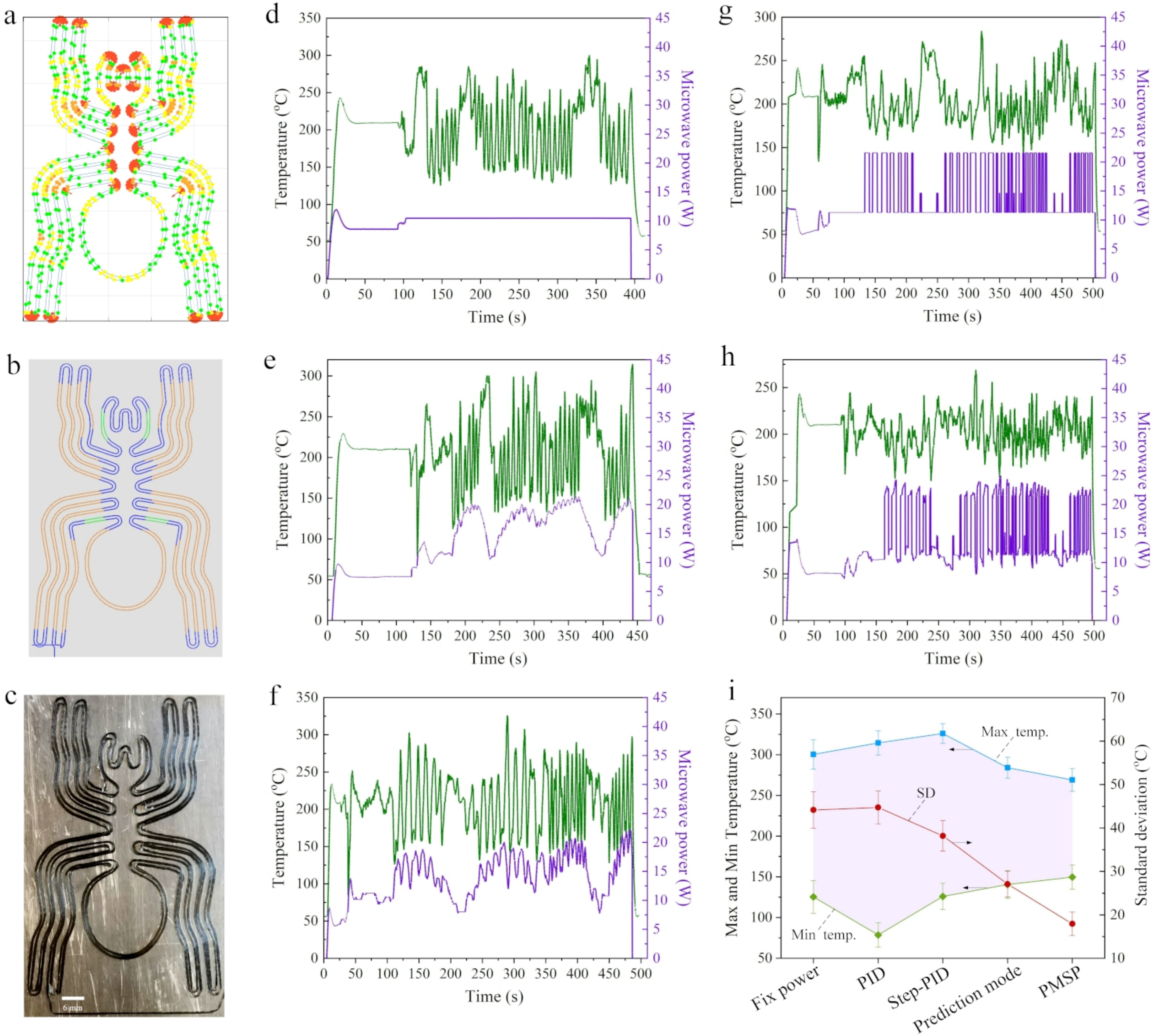

a
b
c
6 mm
d
e
f
g
h
Temperature (°C)
Microwave power (W)
Time (s)
i
Max and Min Temperature (°C)
Standard deviation (°C)
Max. temp.
SD
Min. temp.
Fix power
PID
Step-PID
Prediction mode
PMSP

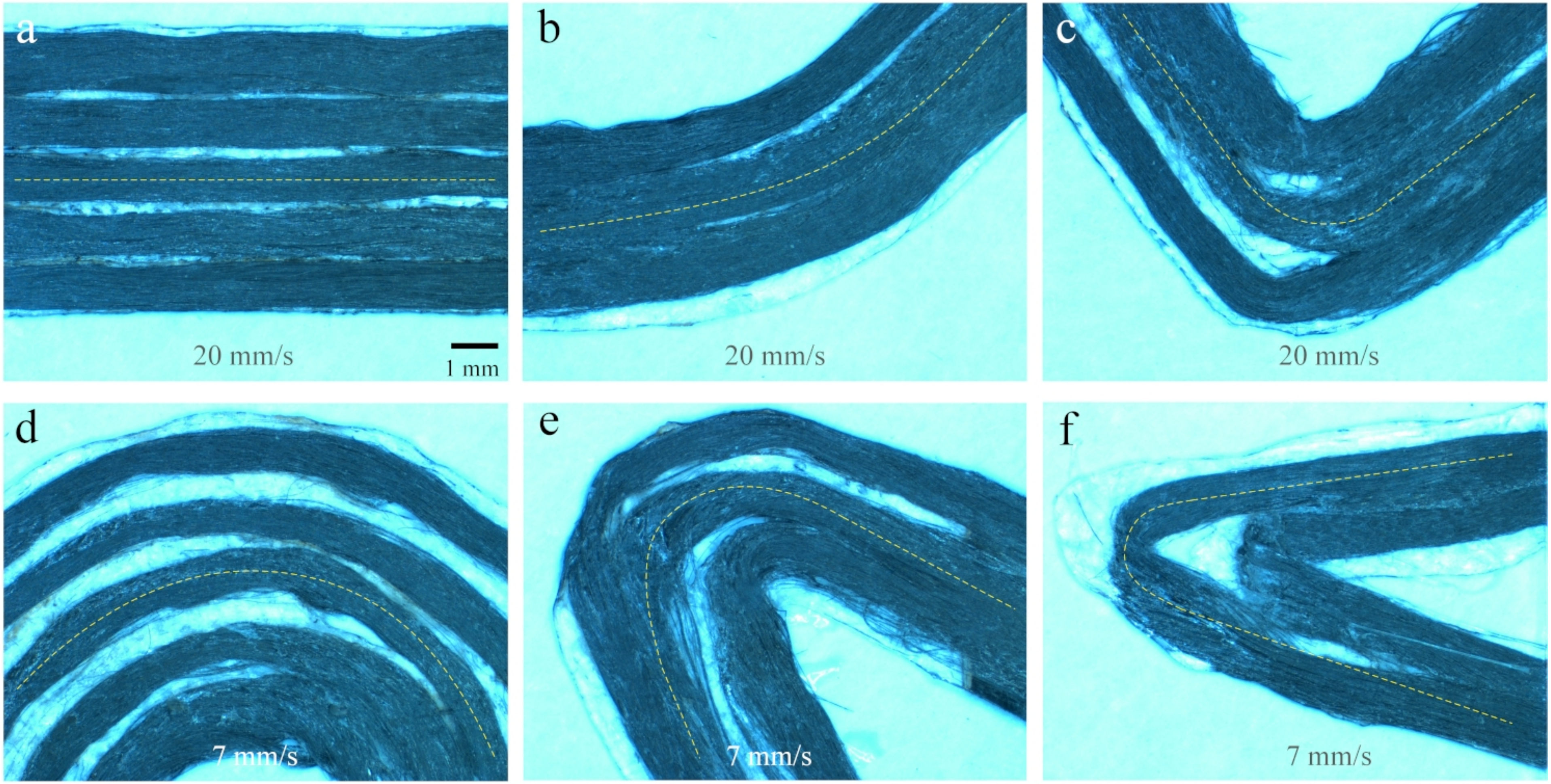
a
20 mm/s
1 mm
b
20 mm/s
c
20 mm/s
d
7 mm/s
e
7 mm/s
f
7 mm/s

Supplementary Information

3D Microwave Printing Temperature Control of Continuous Carbon Fiber Reinforced Composites

Nanya Li*, Guido Link, John Jelonnek

Institute for Pulsed Power and Microwave Technology, Karlsruher Institute of Technology, Eggenstein-Leopoldshafen, 76344, Germany

*Corresponding authors (Nanya.li@kit.edu)

The continuous carbon fiber reinforced polymer (CCFRP) filaments are manufactured in an impregnation system, the schematic diagram of the impregnation system is shown in Fig. S1. Firstly, the continuous carbon fibers are infiltrated by PA845H-PL nylon sizing agent, then drying to remove acetone by pre-heating process (150 ^{o}C). Then the fiber will impregnate the nylon resin under 250 ^{o}C in a small heating chamber (5 mm diameter, 20 mm long). After that, the CCFRP filaments are pulled by the traction fixture and storage in the drum. The positioning devices are applied to keep the carbon fiber in the center of the impregnation heating block. A cooling fan is installed beside the filament and decrease its temperature quickly. The developed impregnation system is shown in Fig. S2. The impregnation system is controlled by a Megatronics board with Marlin firmware.

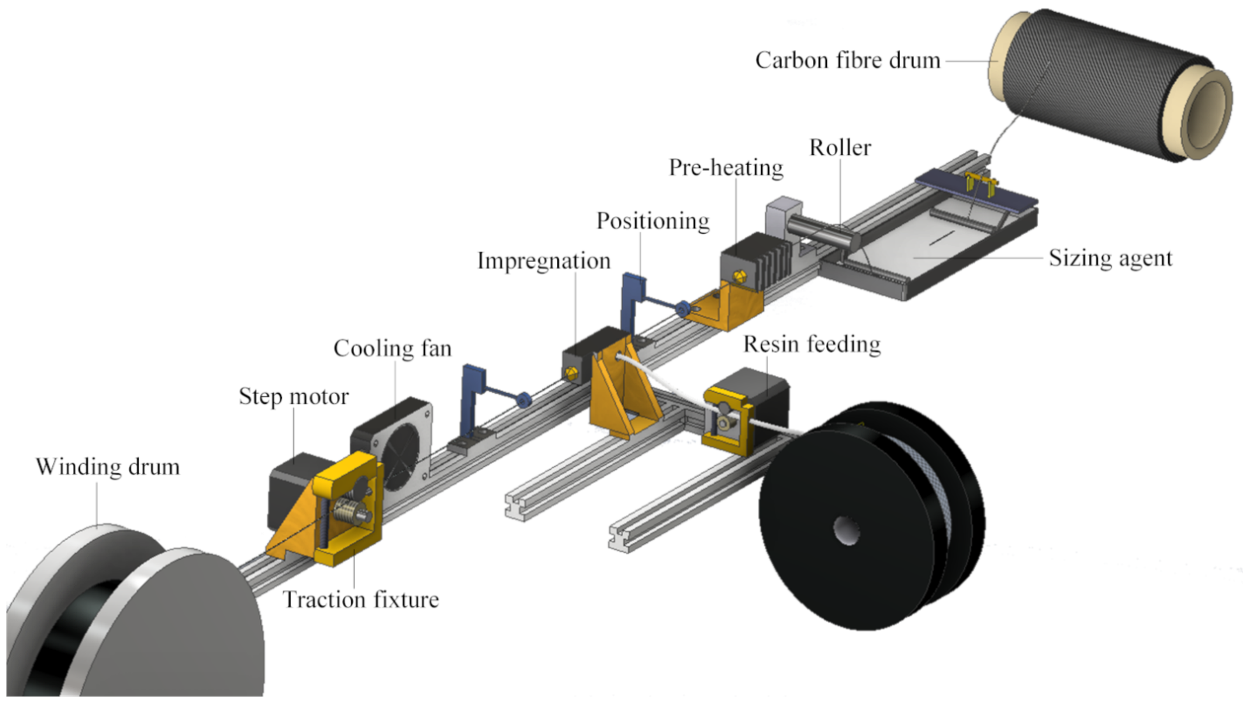

Fig. S1. The schematic diagram of continuous carbon fiber impregnation system to fabricate the CCFRP filament.

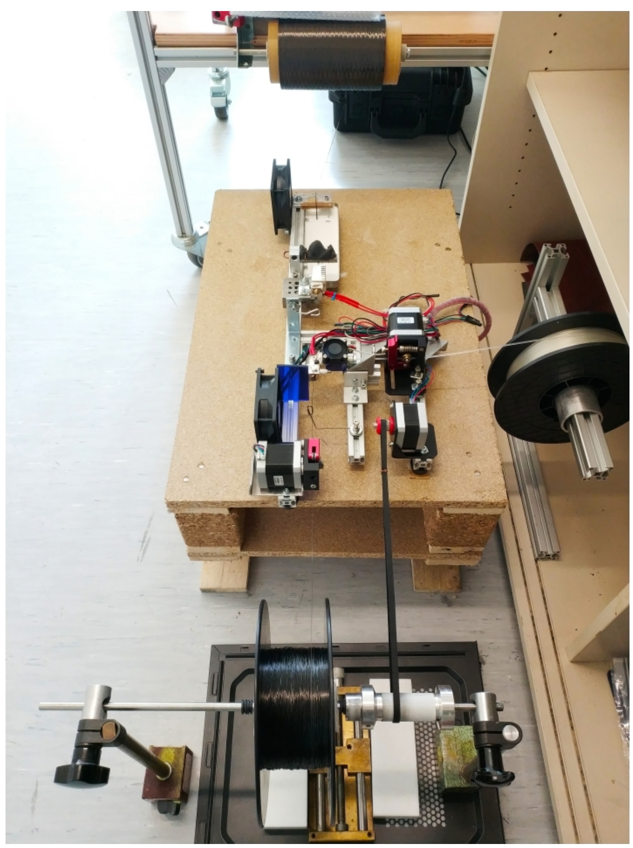

Fig. S2. The developed impregnation system.

The 3D microwave resonant applicator was designed to have an electric field vertical to the CCFRP filaments (TEM mode) to achieve a high penetration depth. The schematic diagram of the microwave printing applicator is shown in Fig. S3 (a). The experimental results exhibit that the 2.45GHz microwave can penetration 5 mm diameter CCFRP filament with 30% fiber volume content. As shown in Fig. S3 (b), the SERPENS has a three-axis motion control system, a resonant applicator is installed in the Z-axis. The printing temperature of the filament is measured by a FLIR A35 infrared camera during the printing process. A 3D microwave printing control system is programmed to control and monitor the printing process.

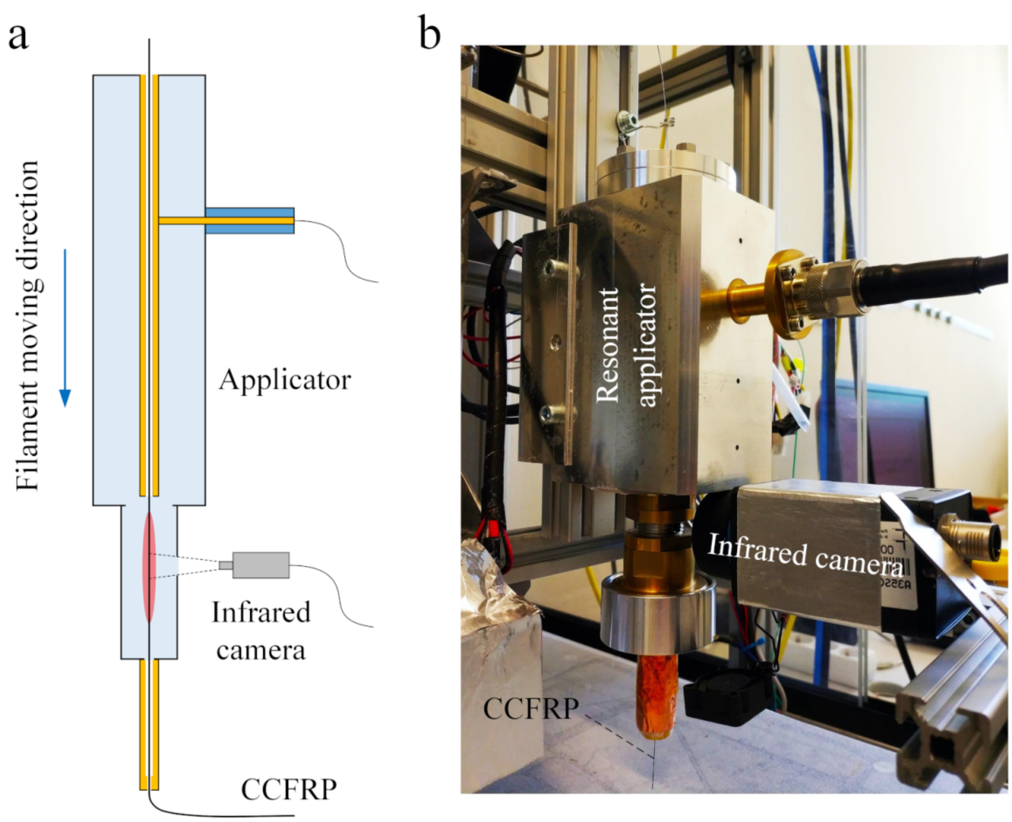

Fig. S3. 3D microwave printer SERPENS of continuous carbon fiber reinforced polymer composites, (a) schematic diagram of the microwave printing applicator, (b) the developed 3D microwave printer.

The schematic diagram of the prediction-model and step-PID (PMSP) control method is shown in Fig. S4. The PMSP algorithm is a closed-loop control system and has the input of trigger signal and temperature data. The output signal directly communicates with the microwave generator and amplifier to control the microwave power. Because there is a communication delay between the PMSP control algorithm and the microwave generator, the prediction-model controller is applied to adjust the microwave power before the changing of the printing speed by detecting a trigger signal. According to the testing results, when the printing speed changes from low speed to high speed, the in advanced compensation time is about 0.4 s, and if the speed change from high to low speed, the compensation time is about 0.7 s. Thus, the G-code is modified to insert M106 (AUX 1 channel output) code before the G1 F (speed control) code, as shown in Fig. S4. Then the Megatronics board output the analog pulse-width modulation (PWM) signal read from the G-code file and convert it to the digital trigger signal. The measured microwave heating temperature of the CCFRP filament by using the FLIR A35 camera will be imported to the PMSP control algorithm.

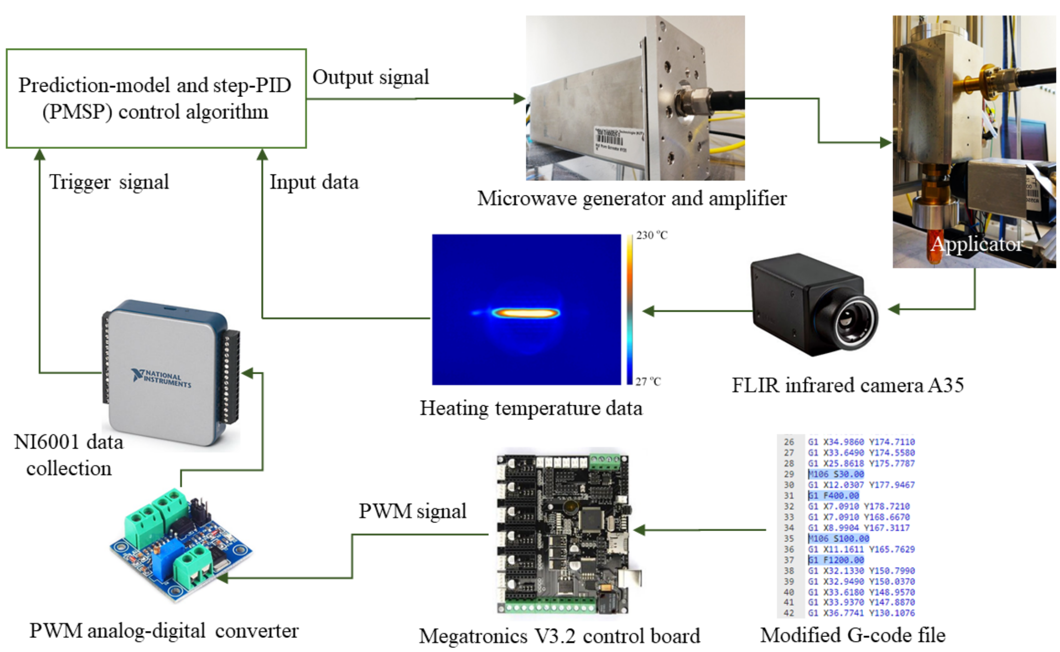

Fig. S4. Schematic diagram of the prediction-model and step-PID (PMSP) control algorithm.

For the modified G-code generation method, three factors are considered to determine the printing speeds of the printing path, including the length of the straight line or curve, the radius of curvature of the curve and the angle between the adjacent direction vectors. Firstly, the original G-code files are imported and loaded as coordinates. Secondly, long straight lines (length >25 mm) and long curves (length >25 mm, the radius of curvature >10 mm) are recognized and extracted to mark as high printing speed path. Secondly, the printing speed of other paths between long lines and long curves are determined with their angle, length and radius of curvature. Also, the compensation time of the communication delay is considered, the in advanced of 0.4 s and 0.7 s are added during the speed changing process. The microwave powers which should be outputted at different printing speed are calculated based on the relationship between the microwave power and the printing speed. Finally, the modified G-code file is generated and used to the PMSP 3D microwave printing temperature control. The corresponding relationship between the printing speeds and the three factors is shown in Table S1.

Table S1. The corresponding relationship between the printing speeds and the three factors.

Printing speed	**Length (mm)**	**Angle (°)**	**Radius of curvature (mm)**
Low (7 mm/s)	/	> 90	≤ 5
Middle (13 mm/s)	$< 25 \& \geq 15$	$\geq 60 \& \leq 90$	$> 5 \& \leq 10$
High (20 mm/s)	≥ 25	< 60	> 10

The calculated angles between adjacent direction vectors of the spanner specimen are shown in Fig. S5. It is obvious that the angles are recognized precisely along the printing path. The relationship of radius of curvature and length of the printing path of the aircraft specimen is shown in Fig. S6. The printing path of the aircraft has three reduplicative paths with 0.5 mm distance of each. Therefore, the period radius of curvature appears along the printing path. As illustrated in Fig. S7, the printing paths of the spider have varying direction vectors and the length of the arrow exhibit the amplitude of the vectors.

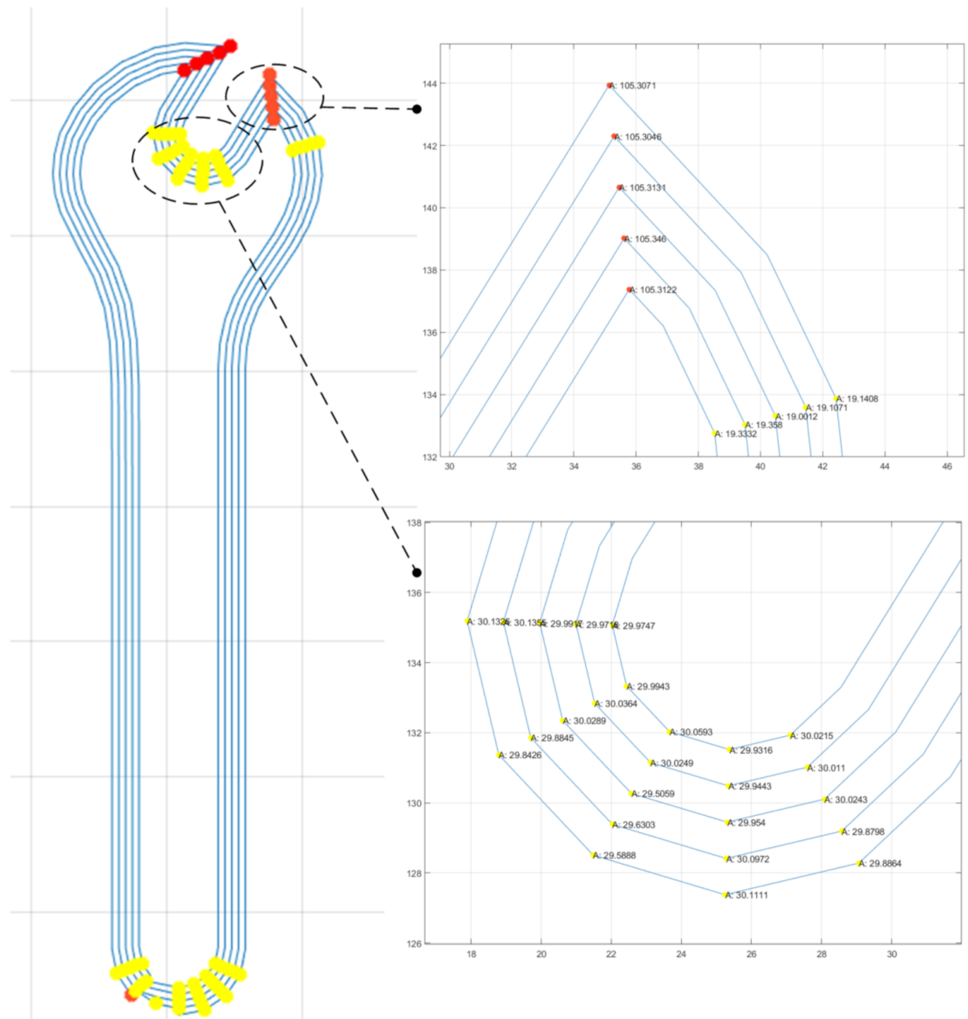

Fig. S5. The calculated angles of adjacent lines of the spanner specimen.

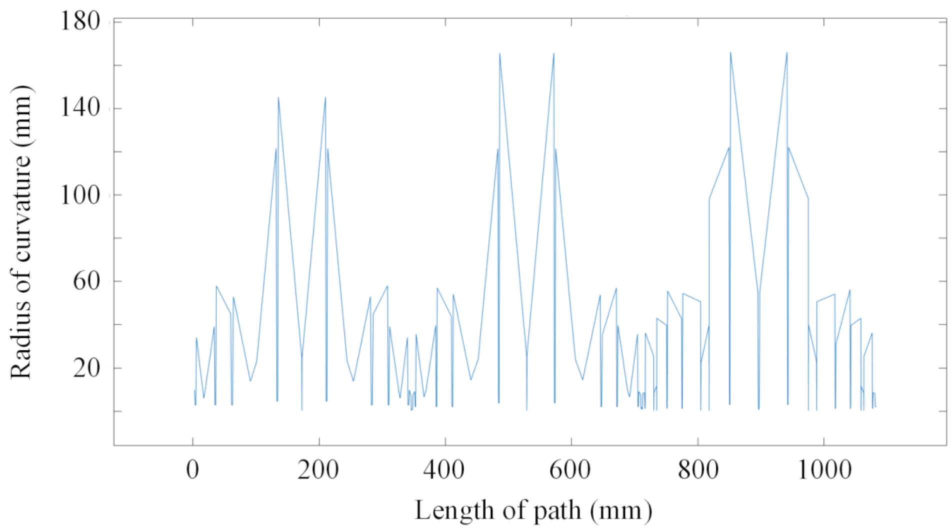

Fig. S6. The relationship of radius of curvature and length of the printing path of the aircraft specimen.

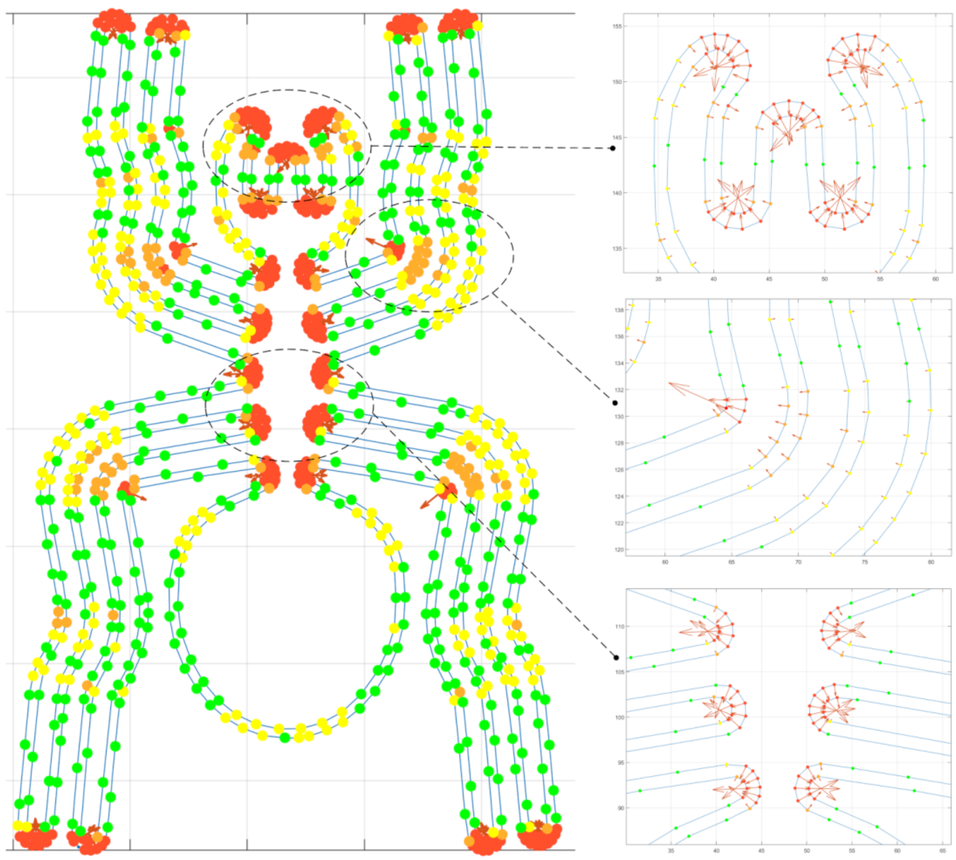

Fig. S7. The calculated radius of curvatures of the Nazca lines spider.

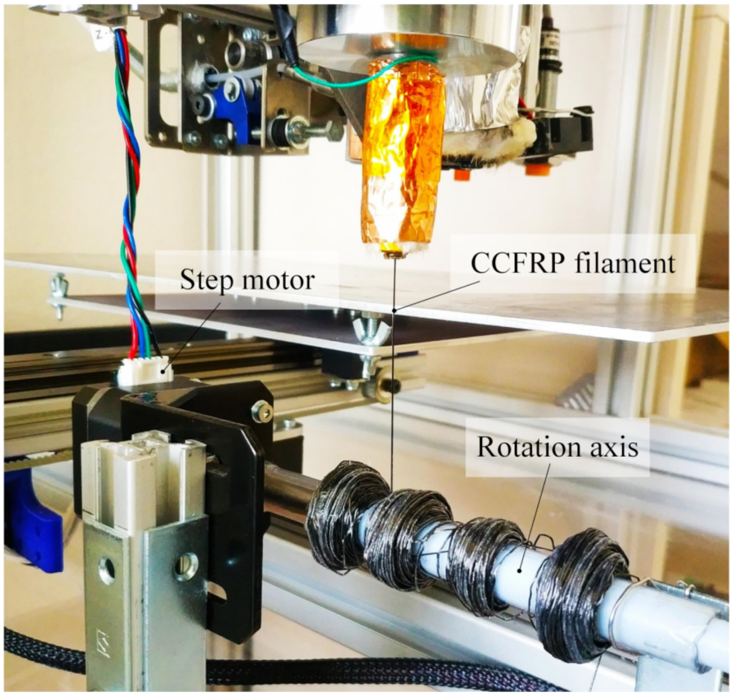

Fig. S8. The 3D microwave printing speed testing device.

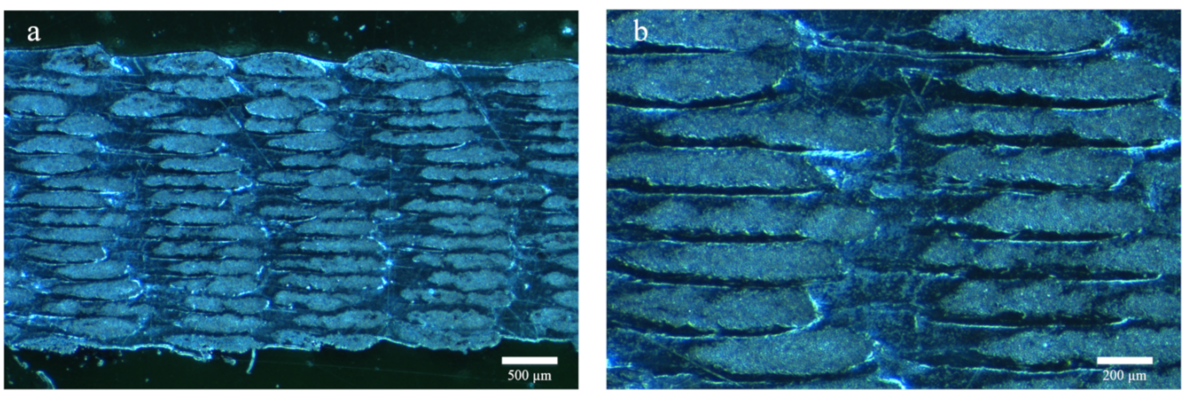

Fig. S9. The cross-section of 3D microwave printed CCFRP specimens, (a) the CCFRP specimens with 16 layers, (b) the zoomed figure of the printed filaments.